Intramolecular Ferromagnetism in a Novel Hexanuclear (μ-Hydroxo)(μ-carbonato)copper(II) Bipyridine Complex. Structure of $[Cu_6(bpy)_{10}(\mu\text{-}CO_3)_2(\mu\text{-}OH)_2](ClO_4)_6\cdot 4H_2O$ and of a Dinuclear μ-Carbonato Complex, $[Cu_2(bpy)_4(\mu\text{-}CO_3)](PF_6)_2\cdot 2DMF$

Paul E. Kruger,[†,‡] Gary D. Fallon,[†] Boujemaa Moubaraki,[†] Kevin J. Berry,[§] and Keith S. Murray*,[†]

Department of Chemistry, Monash University, Clayton, Victoria 3168, Australia, and Westernport Secondary College, Hastings, Victoria 3915, Australia

Received April 6, 1995[⊗]

A novel hexanuclear copper(II) complex, $[Cu_6(bpy)_{10}(\mu\text{-}CO_3)_2(\mu\text{-}OH)_2](ClO_4)_6\cdot 4H_2O$, (**1**, bpy = 2,2′-bipyridine), has the following crystallographic data: triclinic, space group $P\bar{1}$, a = 18.330(5) Å, b = 13.497(3) Å, c = 13.790(8) Å, α = 119.26(2)°, β = 98.96(4)°, γ = 104.19(2)°, Z = 1, V= 2728(2) Å^3. The structure of **1** is made up of discrete centrosymmetric hexanuclear units in which a central planar bis(μ-hydroxo)copper(II) bipyridine moiety contains two *cis*-Cu(bpy)$_2$ fragments attached via carbonate bridging groups, *trans*-axially, to the central Cu atoms. Viewed along the central plane, the bpy rings are arranged in a parallel fashion due to $\pi-\pi$ interactions. Detailed magnetic studies on **1**, over the temperature range 2−300 K and field range 0.1−3.0 T, show that ferromagnetic coupling of the spins on each Cu(II) center occurs, leading to a S = 3 ground state. Application of an appropriate Heisenberg spin-coupling model led to a good fit of the susceptibility and isofield magnetization data with a J value for the central $Cu_2(OH)_2$ moiety of +24 cm^{-1} and J values, for the three identifiable $Cu_2(\mu\text{-}CO_3)$ pathways, in the range +2.75 to + 3.3 cm^{-1}. The corresponding zero-field spin-ladder of energy levels show that the low-lying S levels are within a few wavenumbers of the ground S = 3 level. The consequent M_S Zeeman level population leads to a maximum in the moment versus temperature plot, at *ca.* 4 K, which varies in size and shape as a function of applied field. A second complex, **2**, was formed on recrystallization of the PF_6^- salt of **1** from dimethylformamide. It is binuclear, with formula $(Cu_2(bpy)_4(\mu\text{-}CO_3)](PF_6)_2\cdot 2DMF$ and has the following crystallographic data: **2**, triclinic, space group $P\bar{1}$, a = 9.461(1) Å, b = 11.282(2) Å, c = 12.742(2) Å, α = 99.78(2)°, β = 96.83(1)°, γ = 97.19(1)°, Z = 1, V = 1316.1(4) Å^3. The structure of **2** reveals a unique *anti−anti* mode of carbonate bridging and a separation of 5.26 Å between the two square−pyramidally coordinated Cu atoms. The bridging CO_3^{2-} group and the DMF solvate molecules show structural disorder. In contrast to **1**, this complex displays antiferromagnetic coupling with a J value of −70.2 cm^{-1} (i.e., singlet−triplet splitting of 140.4 cm^{-1}).

Introduction

Considerable interest has developed in recent years in devising ways of making new magnetic molecular materials.[1] Molecular ferromagnets, for example, which display spontaneous magnetic ordering at temperatures below the Curie temperature, T_c, have been obtained using crystalline organic radical,[2] metal complex−organic radical,[3] organometallic charge transfer,[4] and mixed-metal ferrimagnetic chain[5] building blocks. Another tactic which is being developed in a number of laboratories is to synthesize high nuclearity spin coordination−metal clusters that can ultimately be stitched together to form 3-dimensional arrays capable of displaying long-range magnetic ordering.[5−7] The authors of two recent textbooks on magnetochemistry have summarized the present state of knowledge in this exciting area of new materials.[8,9] Spin-coupled clusters with ground-state spins as high as S = 10 have been obtained using oxo-bridged Mn_{12}[10] and Fe_8[11] species, while a S = 12 state was obtained in a hexanuclear Mn(II) complex−organic radical cluster.[6,12] Recently synthesized Fe_{19} hydroxo clusters show even larger spin states.[6,13] Many of these clusters exhibit what has been termed spin frustration; that is they do not display the full degree of spin alignment in the ground state of which they are capable because of competing exchange pathways with different J values.[7,8]

[†] Monash University.
[‡] Present address: School of Chemistry, Queens University, Belfast BT9 5AG, U.K.
[§] Westernport Secondary College.
[⊗] Abstract published in *Advance ACS Abstracts,* August 15, 1995.

(1) Gatteschi, D., Kahn, O., Miller, J. S., Palacio, F., Eds. *Magnetic Molecular Materials*; Kluwer Academic Publishers: Dordrecht, The Netherlands, 1991.
(2) Chiarelli, R.; Novak, A.; Rassat, A.; Tholence, J. L. *Nature* **1993**, *363*, 147.
(3) (a) Gatteschi, D. *Adv. Mater.* **1994**, *6*, 635. (b) Stumpf, H. O.; Ouahab, L.; Bergerat, P.; Kahn, O. J. *Am. Chem. Soc.* **1994**, *116*, 3866.
(4) Miller, J. S.; Epstein, A. J. *Angew. Chem., Int. Ed. Engl.* **1994**, *33*, 385.
(5) Stumpf, H. O.; Pei, Y.; Kahn, O.; Sletten, J.; Renard, J. P. *J. Am. Chem. Soc.* **1993**, *115*, 6738.
(6) Gatteschi, D.; Caneschi, A.; Pardi, L.; Sessoli, R. *Science* **1994**, *265*, 1054.
(7) Schake, A. R.; Tsai, H.-L.; Webb, R. J.; Folting, K.; Christou, G.; Hendrickson, D. N. *Inorg. Chem.* **1994**, *33*, 6020.
(8) Kahn, O. *Molecular Magnetism*; VCH: New York, Weinheim, Germany, and Cambridge, U.K., 1993.
(9) O'Connor, C. J., Ed. *Research Frontiers in Magnetochemistry*; World Scientific: Singapore, **1993**.
(10) Sessoli, R.; Tsai, H.-L.; Schake, A. R.; Wang, S.; Vincent, J. B.; Folting, K.; Gatteschi, D.; Christou, G.; Hendrickson, D. N. *J. Am. Chem. Soc.* **1993**, *115*, 1804.
(11) Delfs, C.; Gatteschi, D.; Pardi, L.; Sessoli, R.; Wieghardt, K.; Hanke, D. *Inorg. Chem.* **1993**, *32*, 3099.
(12) Caneschi, A.; Gatteschi, D.; Laugier, J.; Rey, P.; Sessoli, R.; Zanchini, C. *J. Am. Chem. Soc.* **1988**, *110*, 2795.
(13) (a) Heath, S. L.; Powell, A. K. *Angew. Chem., Int. Ed. Engl.* **1992**, *31*, 191. (b) Day, P. *Science* **1993**, *261*, 431.

0020-1669/95/1334-4808$09.00/0

In the present paper we describe a novel hexanuclear copper(II) bipyridine complex, $[Cu_6(bpy)_{10}(\mu\text{-}CO_3)_2(\mu\text{-}OH)_2](ClO_4)_6 \cdot 4H_2O$ (**1**), in which two central Cu^{II}bpy moieties are bridged by hydroxo groups and each Cu is attached to two other $[Cu^{II}(bpy)_2]$ fragments by bridging carbonate groups. The six spin centers are ferromagnetically coupled, thus giving a ground state of $S = 3$. A detailed field and temperature dependent study of magnetization is described. Complex **1** was first obtained, accidentally, when $[Cu^{II}(bpy)_2]$ groups were being used as "end blockers" in an attempt to make a linear tetranuclear μ-oxamido complex, the carbonate group originating from atmospheric CO_2. Complex **1** was then readily obtained upon reaction of $Cu(OH)_2$, bipyridine, and $NaClO_4$ in air, using the appropriate mole ratio of reagents. Among the many known Cu–bpy species, it is surprising that this compound has not been described before. A binuclear μ-carbonato complex, $[(Cu(bpy)_2)_2(\mu\text{-}CO_3)](PF_6)_2 \cdot 2DMF$ (**2**), was also isolated upon slow recrystallization of the hexanuclear PF_6^- salt from *N,N*-dimethylformamide solution. In contrast to **1**, it shows antiferromagnetic coupling and has an *anti–anti* disposition of the two Cu atoms in relation to the two adjacent oxygen atoms of the bridging carbonate moiety.

Experimental Section

Materials. Solvents were of laboratory grade and were used as received. The salts $NaClO_4 \cdot H_2O$, NH_4PF_6, and $NaPF_6$ were from Aldrich Chemical Co., and 2,2′-bipyridine was from Univar. $Cu(OH)_2$ was prepared by a published method[14] and stored in a desiccator.

Synthesis of $[Cu_6(bpy)_{10}(\mu\text{-}CO_3)_2(\mu\text{-}OH)_2](ClO_4)_6 \cdot 4H_2O$ (1). A methanolic solution (20 mL) containing 2,2′-bipyridine (2.66 g, 17.0 mmol) was added, in air, to a vigorously stirred aqueous suspension of $Cu(OH)_2$ (1.0 g, 10.2 mmol). After several minutes, solid $NaClO_4 \cdot H_2O$ (1.44 g, 10.2 mmol) was added to the suspension, resulting, after several more minutes, in slight darkening of the solution. Stirring was continued for a further 2 days, after which time the mixture was filtered to remove a microcrystalline aqua-colored solid, and the remaining aqua-colored filtrate was set aside. The solid was washed with methanol (2×, 40 mL) and diethyl ether (2×, 100 mL) and dried *in vacuo*. Anal. Calcd for a tetrahydrate $C_{102}H_{90}Cl_6Cu_6N_{20}O_{36}$: C, 44.3; H, 3.3; N, 10.1; Cl, 7.7. Found: C, 44.2; H, 2.9; N, 10.1; Cl, 7.9. *Visible* spectrum (CH_3CN): λ_{max} 656 nm (ϵ = 264 M^{-1} cm^{-1}). μ_{eff}(295 K) = 1.99μ_B(per Cu). Crystals suitable for an X-ray diffraction study were obtained from the filtrate, on standing.

$[Cu_6(bpy)_{10}(\mu\text{-}CO_3)_2(\mu\text{-}OH)_2](PF_6)_6 \cdot 6H_2O$ and $[(Cu(bpy)_2)_2(\mu\text{-}CO_3)](PF_6)_2 \cdot 2DMF$ (2). The hexanuclear complex was prepared in an identical fashion to that of the perchlorate containing species, above, by substituting either $NaPF_6$ or NH_4PF_6 in the place of $NaClO_4 \cdot H_2O$. The compound was obtained directly from the reaction mixture as a blue-green microcrystalline solid. Anal. Calcd for $C_{102}H_{94}Cu_6F_{36}N_{20}O_{14}P_6$: C, 39.8; H, 3.0; N, 9.1; P, 6.0. Found: C, 39.8; H, 2.7; N, 9.1; P, 6.0. *Visible* spectrum (CH_3CN): λ_{max} 661 nm (ϵ = 245 M^{-1} cm^{-1}). μ_{eff}(295 K) = 1.95μ_B(per Cu). Recrystallization of the above solid by slow evaporation of a DMF solution yielded green crystals of a different composition, indicated by a single crystal X-ray diffraction study to be (**2**).

Magnetic measurements were made using a Quantum Design MPMS SQUID Magnetometer with powdered samples (*ca.* 30 mg) of the complexes contained in a calibrated gelatine capsule and held in the center of a soda straw which was attached to the end of the sample rod. In the case of the variable field measurements, made at temperatures as low as 2 K, care was taken to check that no anomalous crystallite orientation (torquing effects) was occurring. The derived magnetic susceptibilities are corrected for the diamagnetism of the ligand and counter ion. The EPR spectrum of a neat powdered sample of **1** was measured at a frequency of 9.1 GHz using a Varian E12 instrument fitted with a liquid nitrogen cryostat.

Crystallographic Measurements on Complexes 1 and 2. A dark aqua colored crystal of **1**, suitable for X-ray analysis, was obtained from the filtrate obtained in the synthesis. A transparent aqua colored crystal of **2** was obtained by slow evaporation of a DMF solution of the PF_6^- salt of complex **1**, and it was sealed in a Linderman glass capillary. Crystal data and experimental details are summarized in Tables 1 and S1 (Supporting Information). The programs used for least-squares refinement were those due to Sheldrick (ref 15 for **1** and ref 16 for **2**). In the structure solution of **1**, a direct methods run yielded the positions of the three unique Cu atoms and structural solution proceeded without incident except for the location of the third ClO_4^- moiety. This group appears to be disordered about two sites (which are close to 0, 0, $^1/_2$ and 0, $^1/_2$, $^1/_2$) and is disordered at those sites. Much effort was put into modeling this disorder but without success. The results reported here are from a refinement without this group. Refinement was by full-matrix least-squares employing anisotropic displacement parameters for Cu, Cl, and O for the located ClO_4^- groups and isotropic displacement parameters for all other atoms (single isotropic displacement parameter for hydrogen—which refined to 0.09(2) Å^2—positioned in geometrically idealized positions: C–H, 0.97 Å). At this point (379 variables, 4682 observed data) R was 0.133. The molecule **1** is centrosymmetric, the center of symmetry being located at 0,0,0. The atomic labeling scheme is shown in Figure 1.

The structure of **2** was solved by conventional Patterson and Fourier methods. Final refinement was by full-matrix least-squares employing anisotropic thermal parameters for all non-hydrogen atoms except those in disorder and a single isotropic thermal parameter for hydrogen fixed

Table 1. Crystallographic Details for $(Cu_6(bpy)_{10}(\mu\text{-}CO_3)_2(\mu\text{-}OH)_2](ClO_4)_6 \cdot 4H_2O$ (**1**) and $[Cu_2(bpy)_4(\mu\text{-}CO_3)](PF_6)_2$ 2DMF (**2**)

	1	**2**
formula	$C_{102}H_{90}Cl_6Cu_6N_{20}O_{36}$	$C_{47}H_{46}Cu_2F_{12}N_{10}O_5P_2$
fw	2763.9	1248.0
space group	$P\bar{1}$ (No. 2)	$P\bar{1}$ (No. 2)
a, Å	18.330(5)	9.461(1)
b, Å	13.497(3)	11.282(2)
c, Å	13.790(8)	12.742(3)
α, deg	119.26(2)	99.78(2)
β, deg	98.96(4)	96.83(1)
γ, deg	104.19(3)	97.19(1)
V, Å^3	2728(2)	1316.1(4)
Z	1	1
d_{calc}, g cm^{-3}	1.64	1.58
μ, cm^{-1}	32.8	9.6
T, °C	20(1)	20(1)
crystal size, mm	0.07 × 0.14 × 0.17	0.36 × 0.36 × 0.16
λ, Å	1.5418 (Cu Kα)	0.71073 (Mo Kα)
R^a	0.133	0.059
$R_w{}^b$		0.073

$^a R = \Sigma||F_o| - |F_c||/\Sigma|F_o|$. $^b R_w = \Sigma|F_o - F_c|w^{1/2}/\Sigma|F_o|w^{1/2}$, where $w = [\sigma^2(F_o) + 0.00077F_o^2]^{-1}$.

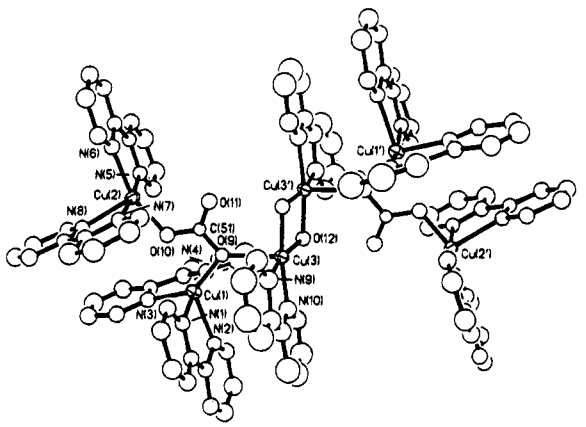

Figure 1. Molecular structure and atomic numbering scheme for **1**. Thermal ellipsoids are shown at the 40% level. Hydrogen atoms are omitted for clarity. ClO_4^- are also not shown.

(14) Brauer, G., Ed. *Handbook of Preparative Inorganic Chemistry;* Academic Press: New York, 1963; Vol. 2, p 1013.

(15) Sheldrick, G. M. *SHELX-76: Program for Crystal Structure Determination.* Cambridge University, England, 1975.

(16) Sheldrick, G. M. *SHELXTL PLUS*, Revision 3.4, Siemens Analytical X-ray Instrument, Inc:, Madison, WI, 1988.

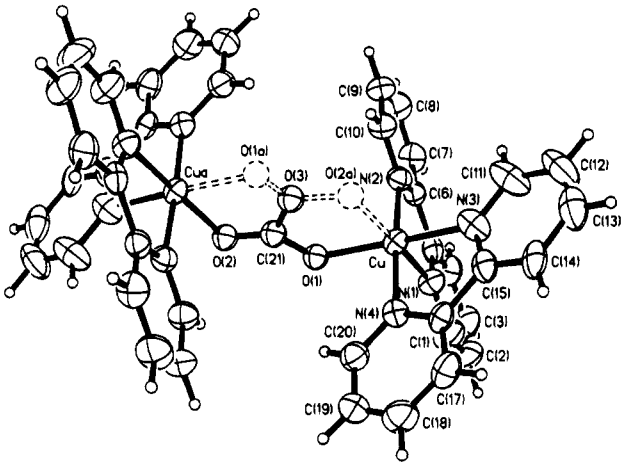

Figure 2. Molecular structure and atomic numbering scheme for **2**. Thermal ellipsoids are shown at the 40% level, whereas all hydrogen atoms are drawn with spheres of arbitrary radius. The mode of disorder of the carbonate is shown.

Table 2. Final Atomic Fractional Coordinates[a] and Equivalent Isotropic Displacement Parameters[b] for Significant Atoms of **1**

atom	x	y	z	U(Iso),[b] Å^2
Cu(1)	0.2677(2)	0.0319(3)	0.0633(3)	0.039(2)
Cu(2)	0.1889(2)	−0.2490(3)	0.1411(1)	0.036(2)
Cu(3)	0.0718(2)	0.1021(3)	0.0823(3)	0.037(2)
C(51)	0.1465(12)	−0.0887(19)	0.0981(18)	0.029(5)
N(1)	0.3239(11)	0.1715(17)	0.2348(17)	0.039(5)
N(2)	0.3311(11)	0.1857(17)	0.0491(17)	0.039(5)
N(3)	0.3576(11)	−0.0378(18)	0.0380(17)	0.043(5)
N(4)	0.2263(12)	−0.0827(18)	−0.1118(18)	0.047(5)
N(5)	0.1459(11)	−0.3877(17)	−0.0240(17)	0.038(5)
N(6)	0.1308(11)	−0.3856(17)	0.1609(17)	0.041(5)
N(7)	0.2332(11)	−0.1228(17)	0.3139(17)	0.038(5)
N(8)	0.3138(11)	−0.2406(17)	0.1828(17)	0.038(5)
N(9)	0.1205(14)	0.2166(21)	0.2570(21)	0.061(6)
N(10)	0.1521(13)	0.2401(20)	0.0899(20)	0.056(6)
O(9)	0.1589(8)	−0.0018(13)	0.0780(12)	0.034(4)
O(10)	0.2043(9)	−0.1261(14)	0.1036(13)	0.041(4)
O(11)	0.0838(9)	−0.1296(14)	0.1126(14)	0.045(4)
O(12)	0.0138(9)	0.0138(13)	−0.0833(13)	0.039(4)

[a] Estimated standard deviations in the last significant digits are given in parentheses. [b] U(eq) for Cu, Cl, and O is defined as one-third of the trace of the orthogonalized $\mathbf{U}_{ij}$ tensor, all other atoms having isotropic values.

at 0.08 Å^2—positioned in geometrically idealized positions: CH, 0.96 Å. At convergence (328 variables, 2465 observed data) R was 0.059 and R_w to 0.073. The goodness of fit value ($[\Sigma w(|F_o| - |F_c|)^2/(N_{obs} - N_{param})]^{1/2}$) was 1.69. The highest peak in the difference Fourier synthesis was 0.54 eÅ^{-3}. The structure of **2** consists of discrete dinuclear cations, $[Cu_2(bpy)_4(\mu\text{-}CO_3)]^{2+}$, in which the bridging carbonate is disordered over two sites. Figure 2 shows the mode of carbonate bridging with the disorder. PF_6^- is the counterion, and there is a DMF solvent of crystallization which is disordered over two sites. Figure 2 also shows the atomic labeling scheme for **2**. Final atomic coordinates for **1** and **2** are given in Tables 2 and 3. Pertinent bond lengths and angles are given in Tables 4 and 5. Details of supplementary material are given at the end of the paper.

Results and Discussion

Syntheses and Characterization. As indicated in the Introduction, hexanuclear complex **1** was first obtained from the mother liquor of a reaction aimed at obtaining tetranuclear copper(II) species in which $Cu(OH)_2$, 2,2′-bipyridine, and sodium perchlorate were reacted with a macrocyclic oxamide formed between 1,5-diaminopentan-2-ol and diethyloxalate. An insoluble green-colored copper oxamide compound was filtered off and was not investigated further. The aqua-colored crystals of **1**, which then slowly deposited, showed weak sharp ν(OH)

Table 3. Final Atomic Fractional Coordinates[a] and Equivalent Displacement Parameters[b] for **2**

atom	x	y	z	U(eq), Å^2
Cu	0.20697(10)	0.18715(8)	0.05009(7)	0.0422(4)
N(1)	0.2040(7)	0.3734(5)	0.0511(5)	0.050(2)
N(2)	0.1389(7)	0.2399(6)	0.1914(5)	0.045(2)
N(3)	0.4306(8)	0.1914(6)	0.1006(6)	0.063(3)
N(4)	0.2793(7)	0.1461(5)	−0.0918(5)	0.045(2)
C(1)	0.2441(10)	0.4360(8)	−0.0216(7)	0.069(4)
C(2)	0.2273(12)	0.5572(8)	−0.0182(9)	0.086(5)
C(3)	0.1678(11)	0.6145(8)	0.0646(8)	0.076(4)
C(4)	0.1285(10)	0.5512(7)	0.1422(7)	0.062(4)
C(5)	0.1484(8)	0.4295(6)	0.1341(6)	0.048(3)
C(6)	0.1101(8)	0.3545(7)	0.2125(6)	0.044(3)
C(7)	0.0492(9)	0.3938(8)	0.3008(7)	0.062(4)
C(8)	0.0184(10)	0.3189(9)	0.3716(7)	0.072(4)
C(9)	0.0500(10)	0.2023(9)	0.3499(7)	0.069(4)
C(10)	0.1090(9)	0.1661(7)	0.2597(6)	0.054(3)
C(11)	0.4992(14)	0.2119(8)	0.2010(8)	0.087(5)
C(12)	0.6439(16)	0.2019(9)	0.2234(10)	0.099(6)
C(13)	0.7153(13)	0.1690(9)	0.1415(11)	0.091(5)
C(14)	0.6486(9)	0.1461(7)	0.0375(8)	0.060(4)
C(15)	0.5037(9)	0.1598(6)	0.0192(7)	0.051(3)
C(16)	0.4201(8)	0.1388(6)	−0.0885(6)	0.044(3)
C(17)	0.4785(10)	0.1119(7)	−0.1826(8)	0.065(4)
C(18)	0.3902(12)	0.0895(8)	−0.2810(8)	0.075(4)
C(19)	0.2447(11)	0.0968(8)	−0.2828(7)	0.068(4)
C(20)	0.1948(9)	0.1255(7)	−0.1865(7)	0.056(3)
P	0.8002(3)	0.1516(2)	0.5992(2)	0.063(1)
F(1)	0.6865(13)	0.0432(10)	0.5842(8)	0.247(7)
F(2)	0.9045(12)	0.2667(8)	0.6115(7)	0.211(6)
F(3)	0.8501(11)	0.1384(9)	0.7145(6)	0.174(5)
F(4)	0.7546(10)	0.1614(8)	0.4822(5)	0.167(5)
F(5)	0.9024(11)	0.0705(10)	0.5567(8)	0.206(6)
F(6)	0.6945(9)	0.2272(8)	0.6501(7)	0.168(5)
C(21)	−0.0502(36)	0.0205(26)	−0.0268(24)	0.048(2)
O(1)	0.0002(10)	0.1374(9)	−0.0168(7)	0.045(2)
O(2)	−0.1724(11)	−0.0203(9)	−0.0608(7)	0.047(2)
O(3)	0.0377(22)	−0.0406(16)	0.0184(15)	0.048(2)
C(23)	0.4084(17)	0.3130(13)	0.5214(12)	0.145(5)
C(22)	0.5090(20)	0.4398(15)	0.7073(15)	0.161(6)
C(22′)	0.2511(22)	0.4230(17)	0.6422(17)	0.182(7)
N(5)	0.3921(13)	0.3981(9)	0.6242(9)	0.116(3)
O(4)	0.4691(25)	0.4844(19)	0.7927(18)	0.175(8)
O(4′)	0.2386(22)	0.4628(18)	0.7304(18)	0.152(7)

[a] Estimated standard deviations in the last significant digits are given in parentheses. [b] U(eq) is defined as one-third of the trace of the orthogonalized $\mathbf{U}_{ij}$ tensor.

stretching frequencies at 3620 and 3520 cm^{-1}, attributable to the bridging hydroxo groups in a $Cu_2(OH)_2$ moiety. As well as the bands from bipyridine and ClO_4^-, the IR spectrum also showed two strong bands at 1525 and 1335 cm^{-1} which, in the light of the crystal structure (*vide infra*), are assigned to bridging CO_3^{2-} groups, the latter being formed by prolonged reaction of hydroxo copper(II) species with CO_2 in the air. The hexanuclear complex was amenable to direct synthesis by using a 3:5:3 ratio of $Cu(OH)_2$, 2,2′-bipyridine, and $NaClO_4 \cdot H_2O$, in air over a period of 2 days. The fixation of atmospheric CO_2 by Cu complexes remains an intriguing and not readily predictable phenomenon. Hydroxocopper(II) species of the present kind, or those with trispyrazolylborate co-ligands,[17] form μ-CO_3 compounds. However, when a competing oxoanion such as nitrate is present, then CO_2 fixation may or may not occur and the resulting $Cu_2(\mu\text{-}XO_3)$ fragment, where X = N or C, can be extremely difficult to distinguish by crystallography or analysis, despite the charge difference.[18,19] Two recent ex-

(17) Kitajima, N.; Koda, T.; Hashimoto, S.; Kitagawa, T.; Moro-Oka, Y. *J. Am. Chem. Soc.* **1991**, *113*, 5664.
(18) Menif, R.; Riebenspies, J.; Martell, A. E. *Inorg. Chem.* **1991**, *30*, 3446.
(19) van den Brenk, A. L.; Byriel, K. A.; Fairlie, D. P.; Gahan, L. R.; Hanson, G. R.; Hawkins, C. J.; Jones, A.; Kennard, C. H. L.; Moubaraki, B.; Murray, K. S. *Inorg. Chem.* **1994**, *33*, 3549.

Table 4. Selected Bond Lengths (Å) and Angles (deg) for $[Cu_6(bpy)_{10}(\mu\text{-}CO_3)_2(\mu\text{-}OH)_2](ClO_4)_6{\cdot}4H_2O$ (**1**)

Bond Lengths			
Cu(1)−N(1)	2.03(2)	Cu(3)−N(10)	2.02(3)
Cu(1)−N(2)	2.23(3)	Cu(3)−O(12)	1.92(2)
Cu(1)−N(4)	2.00(2)	Cu(3)−O(12′)	1.93(2)
Cu(1)−N(3)	2.08(2)	Cu(3)−O(9)	2.35(2)
Cu(1)−O(9)	2.00(2)	Cu(1)···Cu(2)	4.403(7)
Cu(2)−N(5)	1.96(2)	Cu(1)···Cu(3)	3.941(5)
Cu(2)−N(6)	2.06(3)	Cu(2)···Cu(3)	5.982(7)
Cu(2)−N(7)	2.00(2)	Cu(3)···Cu(3′)	2.845(5)
Cu(2)−N(8)	2.23(2)	C(51)−O(9)	1.31(4)
Cu(2)−O(10)	1.94(2)	C(51)−O(10)	1.29(3)
Cu(3)−N(9)	2.00(2)	C(51)−O(11)	1.24(3)
Bond Angles			
O(9)−Cu(1)−N(4)	93.2(8)	N(6)−Cu(2)−N(8)	101.6(9)
O(9)−Cu(1)−N(1)	95.0(7)	O(12)−Cu(3)−O(12)	84.9(9)
O(9)−Cu(1)−N(3)	143.5(9)	O(12)−Cu(3)−N(9)	96.6(10)
O(9)−Cu(1)−N(2)	124.1(8)	O(12)−Cu(3)−N(10)	170.8(10)
N(4)−Cu(1)−N(1)	168.5(11)	O(12)−Cu(3)−O(9)	94.2(7)
N(4)−Cu(1)−N(3)	80.3(9)	O(12)−Cu(3)−N(9)	167.8(11)
N(4)−Cu(1)−N(2)	91.0(9)	O(12)−Cu(3)−N(10)	96.0(9)
N(1)−Cu(1)−N(3)	97.6(8)	O(12)−Cu(3)−O(9)	100.8(7)
N(1)−Cu(1)−N(2)	77.7(9)	N(9)−Cu(3)−N(10)	80.6(11)
N(3)−Cu(1)−N(2)	92.0(9)	N(9)−Cu(3)−O(9)	91.2(9)
O(10)−Cu(2)−N(5)	94.4(9)	N(10)−Cu(3)−O(9)	94.6(9)
O(10)−Cu(2)−N(7)	92.5(9)	Cu(1)−O(9)−Cu(3)	129.8(9)
O(10)−Cu(2)−N(6)	159.2(8)	Cu(1)−O(9)−O(51)	105.9(15)
O(10)−Cu(2)−N(8)	99.1(8)	Cu(3)−O(9)−C(51)	123.9(14)
N(5)−Cu(2)−N(7)	173.0(11)	Cu(2)−O(10)−C(51)	115.7(17)
N(5)−Cu(2)−N(6)	80.3(9)	Cu(3)−O(12)−Cu(3′)	95.1(9)
N(5)−Cu(2)−N(8)	99.4(8)	O(9)−C(51)−O(10)	115.2(21)
N(7)−Cu(2)−N(6)	93.7(9)	O(9)−C(51)−O(11)	121.7(24)
N(7)−Cu(2)−N(8)	78.2(8)	O(10)−C(51)−O(11)	123.2(27)

Table 5. Selected Bond Lengths (Å) and Angles (deg) for $[(Cu(bpy)_2)_2(\mu\text{-}CO_3)](PF_6)_2{\cdot}2DMF$ (**2**)

Bond Lengths			
Cu−N(1)	2.103(6)	Cu···Cu(a)	5.26
Cu−N(2)	2.004(6)	Cu(a)−O(2)	1.900(10)
Cu−N(3)	2.129(8)	Cu(a)···O(3)	2.632(10)
Cu−N(4)	2.011(6)	C(21)−O(1)	1.325(30)
Cu−O(1)	2.009(9)	C(21)−O(2)	1.189(32)
Cu···O(3)	2.792(10)	C(21)−O(3)	1.289(39)
Bond Angles			
O(1)−Cu−N(1)	94.3(3)	N(2)−Cu−N(4)	176.2(2)
O(1)−Cu−N(2)	88.5(3)	N(3)−Cu−N(4)	78.5(3)
O(1)−Cu−N(3)	164.5(3)	O(1)−C(21)−O(3)	114.0(24)
O(1)−Cu−N(4)	92.8(3)	O(1)−C(21)−O(2)	122.5 (27)
N(1)−Cu−N(2)	78.7(3)	O(2)−C(21)−O(3)	122.7 (26)
N(1)−Cu−N(3)	99.5(2)	Cu−O(1)−C(21)	115.5(15)
N(1)−Cu−N(4)	97.6(3)	Cu(a)−O(2)−C(21)	109.9(17)
N(2)−Cu−N(3)	101.0(3)		

amples confirmed the $Cu_2(\mu\text{-}CO_3)$ formation[18,19] while another retained the NO_3^- group even in the presence of $Cu_2(\mu\text{-}OH)_2$ and excess carbonate, the co-ligand in that case being 2,2′-bipyrimidine.[20] It would appear that a coordinated hydroxo group must react with the electrophilic CO_2 molecule for $Cu_2(\mu\text{-}CO_3)$ formation to occur.[17,21]

The PF_6^- salt of complex **1** was prepared in a manner similar to that of the ClO_4^- salt except that $NaPF_6$ was employed. The aqua-colored polycrystalline product deposited from solution and displayed similar IR peaks to those in the ClO_4^- salt. Both of these hexanuclear compounds showed a broad visible band at *ca.* 660 nm in acetonitrile solution. The X-band EPR spectrum of polycrystalline complex **1** (ClO_4^- salt) at 77 K was rather complicated with lines observed throughout the field range 50−8000 G, the 1000−4000 G region showing the most intensity. No attempt has been made to simulate the spectrum, but the occurrence of multiple resonances is in general accord with the ability to fit the microwave quantum ($h\nu$) into the $\Delta M_S = 1$ (and $\Delta M_S = 2$) energy separation in the closely spaced series of low-lying M_S levels, derived from analysis of the magnetic susceptibility data and shown, later, in Figure 8. An interesting transformation of **1**-PF_6 occurred upon attempted recrystallization using dimethylformamide as solvent. Well formed green crystals of a dinuclear complex, $[(Cu(bpy)_2)_2(\mu\text{-}CO_3)](PF_6)_2{\cdot}2DMF$ (**2**), were isolated upon slow evaporation of the solvent. The formation of this cationic fragment can be regarded as a displacement of this group from the *trans*-axial positions of the $[Cu_2(bpy)_2(\mu\text{-}OH)_2]^{2+}$ central core of **1**.

When **1**-PF_6 was slowly recrystallized from acetonitrile solution, two different crystalline materials were obtained, the green μ-CO_3 dinuclear complex, described above, and the light-blue di-μ-hydroxo complex $[Cu_2(bpy)_2(OH)_2](PF_6)_2$, the latter presumably remaining in solution when DMF was used as solvent. Christou *et al.*[22] have also noted that facile displacement of coordinated carboxylates can occur within a series of copper(II) bipyridine μ-carboxylate complexes.

Crystal Structure of Complex 1 (ClO_4^- Salt). A direct-methods analysis yielded the position of three unique Cu atoms, and structural solution proceeded without incident except for the location of the third perchlorate moiety which is disordered (see Experimental Section). The molecular structure has been determined unambiguously and is shown in Figure 1. The overall molecular geometry of the hexanuclear complex consists of the classical di-μ-hydroxy-bis(bipyridine)copper(II)] species, ligated *trans*-axially at each copper atom by μ-carbonatobis-(bipyridine)copper(II)] moieties. The Cu(3)···Cu(3′) separation of 2.845(5) Å and Cu(3)−O(12)−Cu(3′) bridging angle of 95.1-(9)° fall within the range found for this and similarly coordinated di-μ-hydroxocopper(II) dimers. Square-pyramidal geometry to these central copper atoms is furnished by two nitrogen donors from the coordinated bipyridyl ligand and two oxygen atoms from the bridging hydroxo groups, forming the *cis*-N_2O_2 basal plane, and axially by O(9) from the bridging carbonato species. The copper atom lies 0.18 Å above the basal plane toward O(9). The carbonato oxygen O(9) is further coordinated to Cu(1), forming an asymmetric monatomic bridge between Cu(1) and Cu(3); Cu(3)−O(9) 2.35(2) Å, Cu(1)−O(9) 2.00(2) Å, with a Cu(1)−O(9)−Cu(3) bridging angle of 129.8(9)°. The carbonate is additionally coordinated to Cu(2) through O(10), forming a triatomic bridge between Cu(1) and Cu(2) (*syn, anti*) and likewise between Cu(3) and Cu(2) (*anti, anti*). This bridging disposition results in the copper atoms adopting to triangular (scalene) arrangement, with metal−metal separations of Cu(1)−Cu(2) 4.403(7), Cu(1)−Cu(3) 3.941(5), and Cu(2)-Cu(3) 5.982(7) Å (Figure 3a). The centrosymmetric nature of the complex results in the above array being repeated at Cu(1′), Cu(2′) and Cu(3′). Further bond lengths and angles may be found in Table 4.

Coordination around Cu(1) and Cu(2) is best described as being square-pyramidal with distortion toward trigonal bipyramidal. Cu(1) experiences a more pronounced distortion than does Cu(2). The distorted basal planes are N_3O (three bpy nitrogens and carbonato oxygen) in character with the fourth bpy nitrogen occupying the elongated axial position. The least-squares planes formed by each bipyridyl ligand are rotated with respect to each other by 87.2° and 84.5°, for Cu(1) and Cu(2), respectively. Analysis of the shape determining angles using

(20) De Munno, G.; Julve, M.; Lloret, F.; Faus, J.; Verdaguer, M.; Caneschi, A. *Inorg. Chem.* **1995**, *34*, 157.
(21) Palmer, D. A.; van Eldik, R. *Chem. Rev.* **1983**, *83*, 651.
(22) (a) Perlepes, S. P.; Libby, E.; Streib, W. E.; Folting, K.; Christou, G. *Polyhedron* **1992**, *11*, 923. (b) Perlepes, S. P.; Huffmann, J. C.; Christou, G. *Polyhedron* **1992**, *11*, 1471.

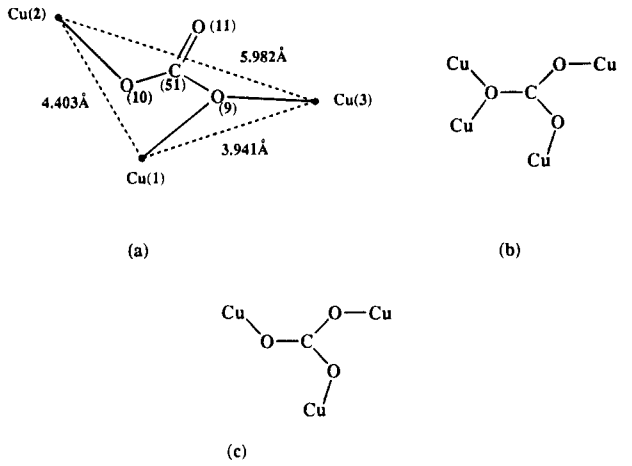

Figure 3. Schematic representation of copper−carbonate units found in (a) complex **1**, (b) malachite, and (c) azurite.

the approach of Reedijk and co-workers[23] yields τ values of 0.41 ± 0.1 and 0.23 ± 0.1 for Cu(1) and Cu(2), respectively (τ = 0 and 1 for perfect square-pyramidal and trigonal-bipyramidal geometries, respectively). The corresponding τ value for the square-pyramidally disposed Cu(3) atom is 0.05 ± 0.01.

A survey of the Cambridge Crystallographic Data Base[24] indicated that the carbonate anion can adopt ten different coordination modes, eight of which are bridging.[21,25] The bridging mode adopted by this group in **1** is unique. The copper atom array and carbonato bridging disposition most closely resembles those found within the copper containing minerals malachite[26] [$Cu_2(OH)_2(CO_3)$] and azurite[27] [$Cu_3(OH)_2(CO_3)_2$], although within these compounds all the oxygen atoms from the carbonate groups are involved in coordination (Figure 3). The hydroxide ions within these minerals further link the copper−carbonato centers into infinite networks.

The influence of bpy-bpy π-stacking interactions has been considered to play a role in determining molecular structure.[28] Inspection of the bipyridine rings incorporating N(9)−N(10) and N(1)−N(2) and coordinated to Cu(3) and Cu(1), respectively, shows that they are essentially parallel to each other. The dihedral angle between these bpy rings is 4.4°, and the separation between them at closest contact is ~3.4 Å. Christou *et al.*[22] obtained similar values within a dinuclear Cu^{II} μ-acetato complex containing bpy rings in *syn*-disposition. These π aromatic ring stacking interactions may play a role in determining the molecular structure in the present complex, and thus favor its formation.

Crystal Structure of Complex 2. As indicated in the Experimental Section the bridging carbonate is disordered over two sites, and this is shown in Figure 2. Disorder in bridging carbonate structures is a reasonably common phenomenon.[18,25] The bridging carbonate adopts an *anti− anti-* disposition which is similar to that found in the dinuclear Cr(III) complex [(Cr(cyclam)$(NH_3))_2(\mu$-$CO_3)$], where cyclam is 1,4,8,11-tetraazacyclotetradecane.[29] The bond distances and angles in the Cu(μ-CO_3)Cu bridging moiety of **2** show some similarities to those in the Cu(2)(μ-CO_3)Cu(3) fragment in **1** but show differences

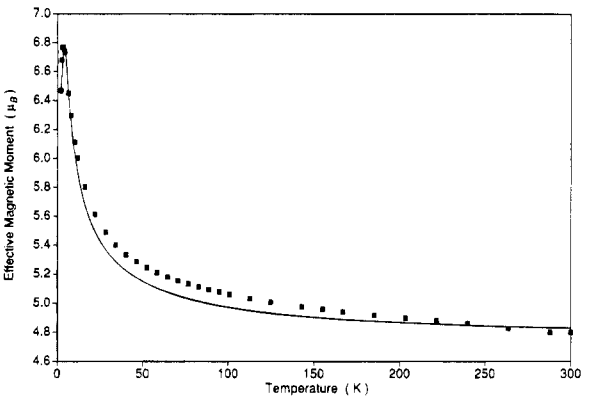

Figure 4. Plot of effective magnetic moment (per Cu_6) versus temperature, for complex **1**. The solid line is that calculated using the model and best-fit parameters shown in eq 2, Figure 7, and Table 6.

to the *syn−anti*-bridged Cu(1)(μ-CO_3)Cu(2) fragment of **1**, particularly with respect to the Cu−O−C angle. It seems reasonable to assume that **2** is obtained from the $(bpy)_2$Cu(1)-(μ-CO_3)Cu(2)$(bpy)_2$ fragment of **1**, upon recrystallization in DMF and thus involves a change from *syn−anti-* to *anti−anti-* coordination. The Cu··Cu separation correspondingly increases to 5.16 Å. There are a large number of known examples of μ-carbonato bridged Cu^{II} complexes,[21,25] and none, to our knowledge, show precisely the present features, although a macrobicyclic complex comes close.[18] The coordination geometry around Cu in **2** is close to square-pyramidal with a basal plane made up of CuO(1)N(2)N(3)N(4) and an apical direction of Cu−N(1).

Magnetic Properties of 1 (ClO_4^- Salt). In a small spin-coupled cluster of the type found in **1** it is important to define the spin state of the ground state and to deduce the nature of the exchange interaction(s) which give rise to the ground-state and to the "spin-ladder" of energy levels.[8,9] We have used variable field magnetization measurements between 2 and 10 K and Brillouin function calculations at 2 K to define the ground state. We had noted the importance of such measurements, some years ago, in defining the ground state of mono- and polynuclear Mn(III) compounds.[30] Other groups have also used multifield data to obtain the low-lying energy levels in a variety of high nuclearity spin clusters and in metal-proteins.[7,10,31] Variable temperature susceptibility measurements (2−300 K), in combination with Heisenberg−Dirac−Van Vleck calculations of exchange parameters and energy levels, have been used to probe the exchange pathways.

Variable temperature effective magnetic moment data, obtained using an applied-field of 1 T, are shown in Figure 4. The μ value at room temperature is 4.8μ_B(per Cu_6), and this increases gradually before passing through a sharp maximum of 6.77μ_B at 3.5 K, a value close to that expected for a S = 3 ground state ($\sqrt{48}$ μ_B for g = 2.0). This kind of μ vs T plot is, in general, quite common for ferromagnetically coupled dinuclear Cu^{II} species, a maximum in μ at low temperature often being ascribed to either intermolecular antiferromagnetic coupling or to zero-field splitting of the S = 1 ground state. Neither of these reasons applies to the present case, as is clearly demonstrated in the variable-field vs variable-temperature plots of Figure 5. The maximum is simply a result of thermal population of the M_S Zeeman levels which arise from the low-lying spin-coupled S levels 3, 2, 1, etc. (*vide infra*). The separation between and/or mixing of such Zeeman levels varies as a function of the field applied. Thus, there is no maximum

(23) Addison, A. W.; Rao, T.; Reedijk, J.; van Rijn, J.; Verschoor, G. C. *J. Chem. Soc., Dalton Trans* **1984**, 1349.
(24) *Cambridge Crystallographic Data Base*, Cambridge, U.K.
(25) Einstein, F. W. B.; Willis, A. C. *Inorg. Chem.* **1981**, *20*, 609.
(26) Süsse, P. *Acta Crystallogr.* **1967**, *22*, 146.
(27) Gattow, G.; Zemann, J. *Acta Crystallogr.* **1958**, *11*, 866.
(28) Dubler, E.; Häring, V. K.; Scheller, K. H.; Baltzer, P.; Sigel, H. *Inorg. Chem.* **1984**, *23*, 3783.
(29) Bang, E.; Eriksen, J.; Glerup, J.; Mønsted, O.; Weihe, H. *Acta Chem. Scand.* **1991**, *45*, 367.
(30) Kennedy, B. J.; Murray, K. S. *Inorg. Chem.* **1985**, *24*, 1552.
(31) Day, E. P.; Sendova, M. S. In *Research Frontiers in Magnetochemistry*; O'Connor, C. J., Ed.; World Scientific: Singapore, 1993; p 395.

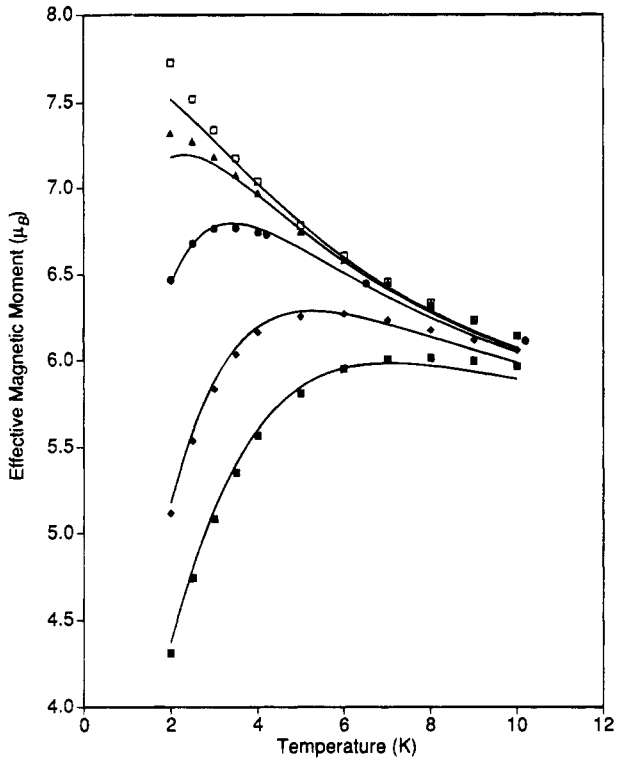

Figure 5. Plots of effective magnetic moment (per Cu_6) of **1** versus temperature (2−10 K) as a function of applied field (field values in tesla: □, 0.1; ▲, 0.5; ●, 1.0; ♦, 2.0; ■, 3.0). The solid lines are the calculated values using the model and best-fit parameters shown in eq 2, Figure 7, and Table 6.

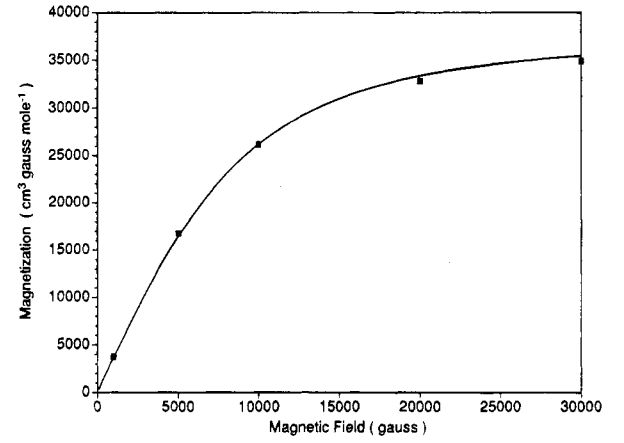

Figure 6. Plot of magnetization versus magnetic field at 2 K for **1**. The solid line is the Brillouin calculation for an $S = 3$ state using eq 1 and $g = 2.205$.

in μ in very low applied fields (e.g. 5×10^{-3} T to *ca.* 0.4 T) in the way that occurs at high fields.

The $S = 3$ ground state was confirmed by calculating the appropriate Brillouin function (eq 1) at 2.0 and 2.5 K and obtaining good fits to the observed magnetization (M) values measured in fields of 0.1, 0.5, 1.0, 2.0, and 3.0 T (Figure 6). The best-fit g value was 2.205.

$$M = \frac{Ng\beta}{2}[7\coth(7\alpha/2) - \coth(\alpha/2)] \qquad (1)$$

$$\alpha = g\beta H/kT$$

The exchange Hamiltonian (eq 2) was used in order to fit the magnetic data and thereby deduce the relevant J values. Fifteen different J values are possible from the structural framework, shown in Figure 7. However, it is possible to reduce

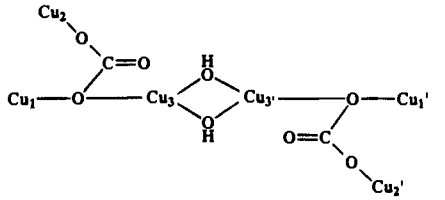

Figure 7. Bridging framework and numbering scheme in **1** used for the exchange model given in eq 2.

Table 6. Best-Fit[a] Exchange Parameters for Complexes **1** and **2**

Hexanuclear Complex **1** (See Figure 7)		
$g = 2.24$	$J_{12} = +2.75$ cm^{-1}	$J_{23} = +2.75$ cm^{-1}
	$J_{13} = +3.25$ cm^{-1}	$J_{33'} = +24.5$ cm^{-1}
Binuclear Complex **2**		
$g = 2.19$	$J = -70.2$ cm^{-1}	% monomer = 8.1

[a] It is difficult and very time consuming to estimate accurately the error bars on the J values in view of the number of parameters involved. When $J_{12} = J_{23}$ was changed by ±0.25 from the value given, the R value for the fit became 20−30% worse ($R = \Sigma|\chi_{obs} - \chi_{calc}|T/\Sigma\chi_{obs}T$), likewise for a similar change in J_{13}. These changes in J_{12} or in J_{13} cause changes in the separation of the higher S energy levels but do not alter their ordering. A lowering in J_{12} lowers the energy separations between the levels. Estimated uncertainties in $g = \pm 0.02$ and in J and $J_{33'} = \pm 0.2$ cm^{-1}.

$$\mathcal{H} = -2\sum_{i=1}^{5}\sum_{j>i}^{6} J_{ij}\bar{S}_i\cdot\bar{S}_j + \sum_{i=1}^{6} g\beta S_i H \qquad (2)$$

this to four parameters in view of the symmetry of the hexanuclear moiety and the nature of the bridging groups.

Thus, the four parameters are

$$J_{12} = J_{1'2'},\quad J_{23} = J_{2'3'},\quad J_{13} = J_{1'3'},\quad J_{33'}$$

All others were assumed zero. An isotropic g value was also assumed. The fitting was achieved by a diagonalization of the 64 × 64 spin wave function matrix under Hamiltonian (2). A g value of 2.24 was quickly found to be appropriate to the 300 K and <10 K μ values. It was held constant while the J values were varied over wide ranges. A unique set of parameter values, shown in Table 6, was found to lead to good fits, particularly in the 2−10 K temperature region, for the five different field values employed (see Figure 5). The zero field spin ladder and the energies of these spin-states in applied fields are shown in Figure 8. When weighting of the levels are considered, in combination with the lower M_S levels from $S = 3$ and the $S < 3$ levels occurring some 18 cm^{-1} above the ground state, it is clear why maxima occur in μ vs T plots at fields greater than *ca.* 0.5 T. The fit in the μ vs T data above 250 K is also good, but the 10−250 K region shows the calculated μ values to be a little lower than those observed. The energies of the levels above the lowest $S = 1$ level are not well determined, and this relates to the uncertainties in the J_{12}, J_{23}, and J_{13} values; see Table 6.

All of the J values are positive, indicative of ferromagnetic coupling in the various bridging pathways. The dominant coupling between Cu_3 and $Cu_{3'}$, has a $J_{33'}$ value similar in size to that observed in dinuclear di-μ-hydroxo complexes such as $[Cu(bpy)(OH)]_2SO_4{\cdot}5H_2O$ ($J = 25$ cm^{-1}).[32] The size and sign of $J_{33'}$ correlates reasonably well[33] with the Cu−O−Cu angle of 95.1. Other recent reports of interest are those by Julve *et*

(32) Crawford, V. H.; Richardson, H. W.; Wasson, J. R.; Hodgson, D. J.; Hatfield, W. E. *Inorg. Chem.* **1976**, *15*, 2107.
(33) Hatfield, W. E. In *Magneto-Structural Correlations in Exchange Coupled Systems*; Willett, R. D., Gatteschi, D., Kahn, O., Eds.; NATO ASI Series 140; Reidel: Dordrecht, The Netherlands, 1985; p 555.

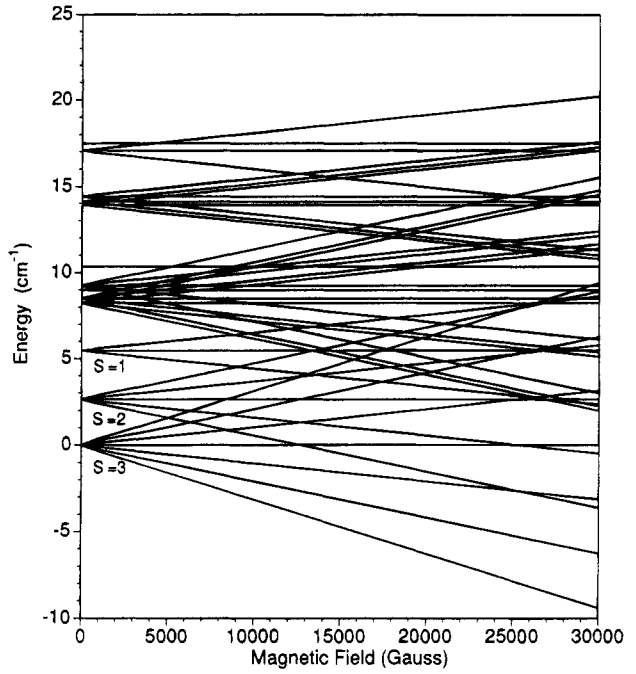

Figure 8. Energy level diagram for complex **1**, in fields up to 3 T, using the best-fit parameter shown in Table 6. The left-hand axis, at zero field, shows the spin ladder of some of the low-lying S states. Crossing of M_S (Zeeman) levels from $S = 3$ and 2 is evident at fields of >0.5 Tesla.

al.[34] on a heptanuclear double-cubane structure found in $[Cu_7(bipyrimidine)_6(OH)_8(H_2O)_2]^{6+}$ in which all seven spins couple ferromagnetically and in which two $J_{33'}$- type constants were found to be $+2.5 \pm 0.1$ cm^{-1}, lower than that found here, and of a tetranuclear (cubane) complex $[Cu_4(OH)_4(bpy)_4](PF_6)_4$ with an $S = 2$ ground state and $J_{33'}$ of $+7.5$ cm^{-1}.[35] Other di-μ-hydroxo bridged copper bipyrimidine chain complexes have shown J values[20] higher than the above-mentioned ones, *viz.*, $+49$ to $+80$ cm^{-1}.

The bridging carbonato pathways lead to small positive J values, similar in size to those observed previously in compounds such as $[(H_2O)CuL]_3(\mu\text{-}CO_3)$ ($J = +5$ cm^{-1}) where L = (((2-(2-pyridyl)ethyl)imino)methyl)pyridine[36] and in $K_2[Cu(CO_3)_2]$ ($J = +1.2$ cm^{-1}), the latter being one of the first known molecular ferromagnets.[37] The $Cu_1\cdots Cu_2$ and $Cu_2\cdots Cu_3$ parameters were found to be equal and both representative of four-bond Cu−O−C−O−Cu pathways. The $Cu_1\cdots Cu_3$ parameter was slightly larger and represents a two-bond Cu−O−Cu pathway.

The dinuclear complex, **2**, displayed typical antiferromagnetic behavior with a maximum in susceptibility occurring at 110 K, and a corresponding and gradual decrease in μ(per Cu), from $1.28\mu_B$ at 295 K to a plateau value of $0.41\mu_B$ below 30 K, the latter due to monomer impurity. The best-fit parameters are given in Table 6. The change in sign of J from the related constant, J_{23}, in **1**, no doubt reflects the different Cu···Cu distance and simultaneous effect of bridging to Cu_1 and Cu_3 (in **1**). Since the O(1) and O(2) atoms of the μ-CO_3^{2-} group, in **2**, are both equatorial oxygen donors, their p-orbitals will overlap with Cu($d_{x^2-y^2}$) magnetic orbitals, and thus antiferromagnetic coupling would be anticipated. However, the non-coplanarity of the two Cu_3NO chromophores would be expected to attenuate the size of J. Sletten *et al.*[38] have also noted the effects that different Cu magnetic orbitals have on the size of J in antiferromagnetically coupled Cu(μ-CO_3)Cu systems in which the carbonato group uses all three oxygen atoms in bridging. Most such examples are very strongly coupled such that diamagnetism is often observed at room temperature.[17,21,25]

Conclusions

The new hexanuclear complex, **1**, joins a growing number of examples of known high-nuclearity spin-coupled clusters. A combination of di-μ-hydroxo and μ-carbonato bridging pathways leads to net ferromagnetic coupling within this cluster. Carbonato bridging groups have not, to date, been as well explored as carboxylato groups in polynuclear species, particularly in regard to their ability to facilitate ferromagnetic superexchange coupling. The precise coordination and bridging mode of the CO_3^{2-} group is important in determining the sign of J in (μ-carbonato)copper(II) clusters, as can be seen in the medium antiferromagnetic coupling displayed by dinuclear complex **2** and the very strong coupling in other recently reported compounds. The μ-hydroxo, μ-carbonato bridging combination also joins other actively studied bridging groups such as μ-oxalato and μ-cyano, employed in small mixed-metal clusters such as $[Cr^{III}\{(\mu\text{-}C_2O_4)Ni^{II}(Me_6\text{-}[14]ane\text{-}N_4)\}_3]^{3+}$ [8,39] and $[Cr^{III}\{(\mu\text{-CN})Ni^{II}(tetren)\}_6](ClO_4)_9$ [40] and in which the orthogonal t_{2g}^3/e_g^2 orbital combination leads to ferromagnetic coupling, with $S = {}^9/_2$ and ${}^{15}/_2$ ground states, respectively.

While the μ-oxalato[41−43] and μ-cyano bridges[44] are proving to be very important in obtaining "3-dimensional" molecular magnetic materials, it remains to be seen if clusters of type **1** can be modified such that the clusters can interact together in an extended manner. Replacing bipyridine with bipyrimidine is one tactic worthy of exploration, although the work of Julve *et al.*,[20,34] mentioned above, suggests that μ-bipyrimidine linkages would lead to antiferromagnetic coupling and hence not to net ferromagnetic ordering. Modification of the parent malachite and azurite structures might be a more profitable exercise.

Acknowledgment. This work was supported by grants from the Australian Research Council to K. S. M.

Supporting Information Available: Tables S1−S10 contain full crystallographic details on **1** and **2**, final atomic fractional coordinates and equivalent isotropic displacement parameters for **1**, anisotropic displacement parameters for Cu, O, and Cl atoms in **1** and **2**, hydrogen atom positional coordinates in **1**, bond lengths and angles for **1** and **2**, and anisotropic displacement parameters for **2** (21 pages). Ordering information is given on any current masthead page.

IC9503949

(34) Real, J. A.; De Munno, G.; Chiappetta, R.; Julve, M.; Lloret, F.; Journaux, Y.; Colin, J.-C.; Blondin, G. *Angew. Chem., Int. Ed. Engl.* **1994**, *33*, 1184.
(35) Sletten, J.; Sorensen, A.; Julve, M.; Journaux, Y. *Inorg. Chem.* **1990**, *29*, 5054.
(36) Kolks, G.; Lippard, S. J.; Waszczak, J. V. *J. Am. Chem. Soc.* **1980**, *102*, 4833.
(37) Gregson, A. K.; Moxon, N. *Inorg. Chem.* **1982**, *21*, 3464.
(38) Sletten, J.; Hope, H.; Julve, M.; Kahn, O.; Verdaguer, M.; Dworkin, A. *Inorg. Chem.* **1988**, *27*, 542.
(39) Pei, Y.; Journaux, O.; Kahn, O. *Inorg. Chem.* **1989**, *28*, 100.
(40) Mallah, T.; Auberger, C.; Verdaguer, M.; Veillet, P. *J. Chem. Soc., Chem. Commun.* **1995**, 61.
(41) Tamaki, H.; Zhong, Z. J.; Matsumoto, N.; Kida, S.; Koikawa, M.; Achiwa, N.; Hashimoto, Y.; Okawa, H. *J. Am. Chem. Soc.* **1992**, *114*, 6974.
(42) Decurtins, S.; Schmalle, H. W.; Schneuwly, P.; Ensling, J.; Gütlich, P. *J. Am. Chem. Soc.* **1994**, *116*, 9521.
(43) Atovmyan, L. O.; Shilov, G. V.; Ovanesyan, N. S.; Pyalling, A. A.; Lyubovskaya, R. N.; Zhilyaeva, E. I.; Morozov, Y. G. *Synth. Met.* **1995**, *71*, 1809.
(44) Mallah, T.; Thiebaut, S.; Verdaguer, M.; Veillet, P. *Science* **1993**, *262*, 1554.